Acta Cryst. (1997). B53, 498–503

The Elusive Crystal Structure of Uric Acid Dihydrate: Implication for Epitaxial Growth During Biomineralization

G. ARTIOLI,[a]* N. MASCIOCCHI[b] AND E. GALLI[c]

[a]*Dipartimento di Scienze della Terra, Universita' di Milano, Via Botticelli 23, I-20133 Milano, Italy,* [b]*Dipartimento di Chimica Strutturale e Stereochimica Inorganica, Universita' di Milano, Via Venezian 21, I-20133 Milano, Italy, and* [c]*Dipartimento di Scienze della Terra, Universita' di Modena, Via S. Eufemia 19, I-41100 Modena, Italy. E-mail: artioli@iummi4.terra.unimi.it*

(Received 28 August 1996; accepted 18 October 1996)

Abstract

The crystal structure of the elusive uric acid dihydrate phase, a known component of human pathological biomineralizations, has been investigated by a combination of synchrotron and conventional X-ray diffraction experiments. $C_5H_4N_4O_3.2H_2O$, orthorhombic, *Pnab*, a = 7.409 (1), b = 17.549 (3), c = 6.332 (1) Å, Z = 4, wR = 0.030 and 0.041 for two independently measured datasets. The molecular packing, encompassing hydrogen-bonded layers of water molecules and statistically disordered organic moieties, fully clarifies on a structural basis the observed epitaxial growth of uric acid dihydrate with associated phases in human stones, such as anhydrous uric acid and whewellite. Synchrotron data confirmed the existence of weak reflections violating the extinction conditions and are interpreted by the presence of short-range ordering of the uric acid molecules at distances of the order of a few adjacent cells.

1. Introduction

Uric acid dihydrate, $C_5H_4N_4O_3.2H_2O$, is a known component of human pathological biomineralizations, especially urinary stones and gout tophus. In human calculi it has long been described associated with anhydrous uric acid, calcium oxalates and sodium urates (Lonsdale & Mason, 1966; Lonsdale, Sutor & Wooley, 1968; Prien & Prien, 1968; Frank, Lazebnik & DeVries, 1970). As an insoluble component together with the anhydrous form of uric acid it is also the common means of nitrogen expulsion from birds and reptiles and it is found as an organic mineral residue in surface deposits (Bridge, 1974; Artioli, Galli & Ferrari, 1993). A number of studies have been performed in the past concerning the identification of uric acid dihydrate as a phase in urinary calculi (Shirley, 1966; Sutor, 1968; Sutor & Scheidt, 1968) and the definition of its crystal morphology and optical properties (Ringertz, 1965). From the cell parameters and knowledge of the commonly developed morphological faces, Lonsdale (1968) postulated that epitaxial growth plays an important role in controlling the nucleation and crystal growth of the phases commonly associated in human stones. The epitaxial growth model has since received much attention (Sutor & Wooley, 1972; Meyer, Bergert & Smith, 1976; Mandel & Mandel, 1980) and it has been experimentally proved between the two forms of uric acid (Boistelle & Rinaudo, 1981) and between anhydrous uric acid and whewellite (Deganello & Coe, 1983). However, epitaxy ought to be justified by structural interpretation and it is at first sight surprising that the crystal structure of uric acid dihydrate, a rather simple molecular compound with important implications for human and animal metabolism, is still unknown.

Several research groups in the past have attempted the full crystallographic study of uric acid dihydrate without success. Ringertz (1965) could not unambiguously determine the space group because different crystals showed inconsistent systematic extinctions, although the optical data and X-ray diffraction patterns confirmed the orthorhombic system. Sutor & Scheidt (1968) cited structural work in progress at the time and they tentatively proposed the *Pnab* (after transformation into the lattice metrics presented later) space group for the compound. No model for the crystal structure is available in the literature to date.

2. Structure analysis and results

Initial diffraction studies were carried out on very small crystals of uric acid dihydrate found on rock surfaces as wash-outs of birds' droppings (Artioli, Galli & Ferrari, 1993). The small crystal dimensions ($100 \times 15 \times 3\ \mu m^3$ on average) did not allow full data collection for the structure solution, although long-exposure X-ray precession photographs allowed confirmation of the cell proposed by Ringertz (1965). More important, the natural crystals proved to be stable at ambient conditions for months, even after prolonged X-ray exposures. This is in agreement with the observation that natural crystals from human bladder stones and from birds' eggs are

known to be stable (Ringertz, 1965), while synthetic crystals of uric acid dihydrate present a relatively rapid phase transformation to the anhydrous form at 298 K (Ringertz, 1965; Boistelle & Rinaudo, 1981; Hesse, Schneider, Berg & Hienzsch, 1975). Partial data collection was also performed on one of the crystals by means of single crystal diffraction using synchrotron radiation. A total of 512 reflections were collected at Lure using a wavelength of 0.6888 Å and the extremely good signal-to-background ratio available on the wiggler line made it possible to observe several weak diffraction peaks violating the extinction conditions of space group *Pnab*. Particularly evident were some reflections (*e.g.* 032) violating the extinction condition of the *n* glide perpendicular to the *a*-cell vector, in agreement with the earlier observations of Ringertz (1965). Weak reflections violating the extinction conditions of the screw axis along **b** and of the *b* glide perpendicular to the *c*-cell vector were also present. The scarcity of diffraction data did not allow the solution of the crystal structure, although the dataset was consistent with the choice of an orthorhombic space group with cell a = 7.41, b = 17.54 and c = 6.34 Å, with the presence of screw diads along the *a* and *c* axes, and of the *a* glide perpendicular to the *b*-cell vector. The extinction conditions are not consistent with an orthorhombic space-group symmetry, in spite of the orthorhombic unit-cell metric, crystal morphology and optical data observed in both natural and synthetic crystals. The lack of consistent space-group symmetry likely caused the failure of previous attempts of structure determination.

At this stage of the work it fortuitously came to our attention the availability of well developed crystals of uric acid dihydrate from human urinary sediments. A patient under treatment for urolithiasis at the City Hospital in Carpi (Modena, Italy) produced well crystallized uric acid dihydrate for a period of several months, because of abnormal metabolism probably induced by a combination of dietary and pharmaceutical conditions. The crystals proved to be chemically and optically homogeneous X-ray diffraction data were in agreement with previous measurement and some of the crystals were large enough for data collection with conventional instruments. Full diffraction datasets were collected on two different crystals using standard measurement conditions. The two datasets were collected with Mo $K\alpha$ radiation: the first using a Nonius CAD-4 instrument and a light yellow crystal (maximum $\sin\theta/\lambda$ = 0.59 Å^{-1}, 2903 measured reflections) and the second using a Kuma KM4 instrument and a bright orange crystal (maximum $\sin\theta/\lambda$ = 0.70 Å^{-1}, 3921 measured reflections). Crystal data: a = 7.409 (1), b = 17.549 (3), c = 6.332 (1) Å, orthorhombic, *Pnab*, Z = 4, M_r = 204.15 g mol^{-1}, D_x = 1.646 g cm^{-3}; $F(000)$ = 424; μ = 1.5 cm^{-1}; maximum difference-Fourier residual (dataset 1) = 0.14 e Å^{-3}. The data were corrected for Lorentz and polarization effects. Due to the small crystal dimensions and the very low absorption coefficient, data were not corrected for absorption effects. Indeed, ψ-scans of suitable reflections having χ values close to 90° indicated variations dictated only by the counting statistics (resulting in fake transmission factors ranging from 0.987 to 1.000).

Although both datasets showed violations of the *Pnab* space group, intensity statistics on 6824 observed reflections indicated that the average $\langle F_o/\sigma(F_o)\rangle$ of the reflections violating the *n*, *a* and *b* glide planes are 2.75, 1.93 and 1.25%, respectively. It was therefore decided to attempt the structure solution in the average, orthorhombic, *Pnab* (non-conventional setting of *Pbcn*, number 60) space group. Dataset 1 was used for structure determination using the *SIR*92 program system (Altomare *et al.*, 1994). A straightforward structure model was determined, based on the molecule of uric acid located on the crystallographic twofold axis along **b**. This model implies a 50% disorder of the organic moiety, which has no internal twofold symmetry, with the five- and six-membered rings statistically superimposed. The external packing-sensitive O, N and H atoms are ordered, while only two atoms (C3 and C4) are needed to be split about the twofold axis. The preliminary structure model was then refined using both available datasets and converged rapidly to acceptable agreement factors, allowing the direct location of the water oxygen and of all the H atoms, including the two independent H atoms linked to the N atoms of the uric acid molecule. Therefore, as in the parent structure of the anhydrous form (Ringertz, 1966), the uric acid molecule is in the triketo form. Refinement using unmerged datasets was then attempted in several orthorhombic and monoclinic crystallographic subgroups of *Pnab*, and particularly those lacking the diad axis along **b** (which is the symmetry element imposing the molecule disorder), those lacking the *n*, *a* or *b* glide planes (which are the apparently unlikely symmetry elements on the basis of the systematic extinction violations), or both. The following space groups were tested: $P2_1ab$, *Pn2b*, $Pna2_1$, $P2_1/n11$, $P12/a1$, $P112_1/b$ and $P2_122_1$. However, none of the refinements in space groups of symmetry lower than *Pnab* could remove the molecular disorder. The model implying twinning of a monoclinic crystal has also been tested and discarded, as it did not improve our final model by removing the disorder.

The final model therefore was chosen as follows: (*a*) space group *Pnab* is believed to satisfactorily describe the average molecular arrangement of uric acid dihydrate; (*b*) the uric acid molecules are linked by hydrogen bonds about inversion centres, such that imidazole rings (I) face each other, as do pyrimidine rings (P) [schematized by the (IP).(PI).(IP) sequence], and generate ribbons running along [102] and [$\bar{1}$02]; (*c*) disorder arises by the energetically equivalent opposite orientation [*e.g.* (IP) *versus* (PI)] of the organic moiety in neighbouring cells, as depicted by

the (PI).(IP).(PI) sequence; (*d*) space-group violations may be ascribed to diffraction effects arising from short-range ordering of the molecules at distances of the order of a few adjacent cells; (*e*) although the anisotropic description of the atomic displacement tensor of the C1 atom (lying on the twofold axis) is slightly distorted by local static effects, the model using a split C1 site resulted in abnormal C—C and C—N bonds, making the one-site model preferred from strict geometrical considerations. As a consequence of disorder, the local geometry involving the split C3 and C4 atomic positions is poorly determined and should be taken only as informative of such disorder. The selected structure model (95 parameters) was then eventually simultaneously refined using both (individually merged) datasets to agreement factors $wR(F) = [\Sigma w(F_o - F_c)^2/\Sigma F_o^2]^{1/2} = 0.030$ and 0.041 for datasets 1 (2601 observed reflections) and 2 (3410 observed reflections), respectively, using anisotropic displacement parameters for all non-H atoms. Individual weights were assigned as $w = 1/\sigma^2(F_o)$, leading to a goodness-of-fit value of 1.42. The *GSAS* program system was used for all calculations (Larson & Von Dreele, 1994). An *ORTEP* drawing of the (disordered) uric acid molecule and its labelling scheme are shown in Fig. 1. Final atomic fractional coordinates and equivalent isotropic displacement parameters are reported in Table 1.*

* Lists of atomic coordinates, anisotropic displacement parameters and structure factors have been deposited with the IUCr (Reference: NA0077). Copies may be obtained through The Managing Editor, International Union of Crystallography, 5 Abbey Square, Chester CH1 2HU, England.

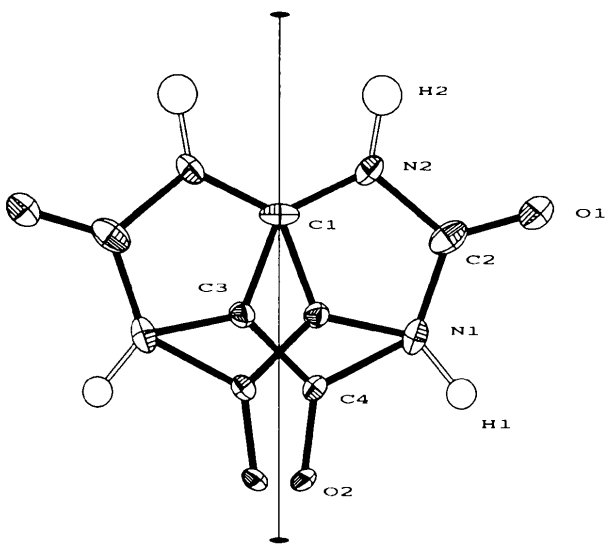

Fig. 1. *ORTEP* (Johnson, 1965) drawing of the (disordered) uric acid molecule, showing the atom-labelling scheme and the statistical twofold axis. Thermal ellipsoids are drawn at the 50% probability level.

Table 1. *Atomic coordinates and displacement parameters for uric acid dihydrate*

$U_{iso}(100 \times Å^2)$ were refined isotropically for H atoms, while they represent the isotropic equivalent factor defined as $(U^{11} + U^{22} + U^{33})/3$ for all atoms refined anisotropically. Starred atoms were refined with half occupancy (see text).

Name	*x*	*y*	*z*	U_{iso}
O1	0.98055 (13)	0.10058 (5)	0.02678 (15)	7.09 (6)
O2*	0.76902 (58)	−0.10385 (7)	0.45256 (33)	4.72 (14)
N1	0.86868 (14)	0.00815 (7)	0.24593 (16)	5.27 (6)
N2	0.83086 (14)	0.13247 (6)	0.33470 (14)	5.01 (7)
C1	3/4	0.09818 (9)	1/2	5.06 (12)
C2	0.90090 (19)	0.08153 (7)	0.18692 (21)	6.20 (11)
C3*	0.78316 (39)	0.02218 (11)	0.43098 (35)	3.82 (17)
C4*	0.78014 (37)	−0.03346 (12)	0.43280 (33)	3.36 (16)
H1	0.9178 (14)	−0.0373 (5)	0.1669 (14)	6.1 (4)
H2	0.8465 (12)	0.1893 (4)	0.3141 (14)	5.0 (4)
O*w*	0.90142 (20)	0.28182 (6)	0.26698 (26)	10.22 (9)
H*w*1	0.8040 (20)	0.3095 (9)	0.2164 (23)	17.2 (9)
H*w*2	0.9272 (22)	0.3057 (9)	0.3979 (17)	20.4 (11)

3. Discussion

The geometries of the uric acid molecule in the crystal of the anhydrous (Ringertz, 1966) and the dihydrate forms are very similar (see Table 2) and the slight differences are directly related to the packing of the molecules *via* the hydrogen-bonding network or, as stated above, to the slight misplacement of the disordered C3 and C4 atoms. As in the crystal of anhydrous uric acid, two adjacent molecules lie in the same plane and are strongly connected by two N—H···O bonds related by inversion centres. These molecules form ribbons parallel to the [102] and [$\bar{1}$02] crystallographic directions, which are perfectly equivalent to those present along the [012] and [01$\bar{2}$] directions of anhydrous uric acid. While in the ribbons of the anhydrous form the centres of symmetry are strictly obeyed, so that imidazole and pyrimidine rings of the uric acid molecule are always connected to the equivalent rings of the adjacent molecule across the centre, in the structure of uric acid dihydrate, given the observed disorder, we cannot discard the possibility that the connection of imidazole and pyrimidine rings across the pseudo-centre of symmetry exists. However, such a symmetry breaking does not occur if the interpretation of the observed diffraction pattern and the disorder discussed above is correct.

The plane ribbons composed of hydrogen-bonded uric acid molecules are directly connected again by N—H···O bonds in the anhydrous form, while they are packed through hydrogen-bonded water molecules in the dihydrate form. The water molecules act as hydrogen-bond acceptors and donors, forming a remarkable network of N—H···O*w* and O*w*—H···O connections and contributing to the crystal packing of the uric acid molecules in the crystal. Fig. 2 shows a projection of the structure of uric acid dihydrate and, for comparison, its analogue in the anhydrous form.

Table 2. *Interatomic distances (Å) and angles (°) in uric acid dihydrate*

The intramolecular distances and angles are compared with the values obtained for the uric acid molecule in anhydrous uric acid (Ringertz, 1966).

Intramolecular bonds

	Uric acid dihydrate	Anhydrous uric acid
N1—C2 (2×)	1.362 (1)	1.367 (5)–1.359 (4)
N1—C3	1.356 (2)	1.387 (5)
N1—C4	1.539 (2)*	1.397 (5)
N1—H1 (2×)	1.010 (8)	
N2—C1 (2×)	1.349 (1)	1.356 (5)–1.360 (4)
N2—C1 (2×)	1.395 (1)	1.382 (4)–1.376 (5)
N2—H2 (2×)	1.011 (7)	
C1—C3	1.424 (2)	1.360 (4)
C2—O1 (2×)	1.221 (1)	1.223 (5)–1.241 (4)
C3—C4	1.385 (2)	1.411 (5)
C4—O2	1.244 (2)	1.233 (4)
C2—N1—C3	98.5 (1)	108.1 (3)
C2—N1—C4	137.3 (2)*	128.8 (3)
C1—N2—C2 (2×)	113.7 (3)	109.2 (3)–118.4 (3)
N2—C1—N2	127.0 (7)	128.3 (3)
N2—C1—C3	137.1 (2)*	124.1 (3)
N2—C1—C3	95.9 (1)	107.5 (3)
N1—C2—N2 (2×)	110.8 (2)	116.0 (3)–107.1 (3)
N1—C2—O1 (2×)	124.9 (1)	122.6 (3)–126.8 (3)
N2—C2—O1 (2×)	124.3 (7)	121.4 (3)–126.1 (3)
N1—C3—C4	124.7 (1)	130.8 (3)
N1—C3—C1	121.1 (4)*	108.0 (3)
C1—C3—C4	114.2 (8)	121.2 (4)
N1—C4—C3	106.9 (3)	111.3 (3)
N1—C4—O2	125.2 (1)	122.3 (3)
C3—C4—O2	147.8 (3)*	126.4 (3)

* These values are not acceptable from a chemical point of view and mainly reflect the misplacement of some atoms due to the statistical disorder about a twofold axis (see text)

Intermolecular bonds (uric acid dihydrate)

A—H···*B*	*A*—H	*A*···*B*	H···*B*	*A*—H···*B*
N1—H1···O1^{i}	1.010 (8)	2.805 (1)	1.818 (8)	165.0 (8)
N2—H2···O*w*	1.011 (7)	2.707 (2)	1.700 (8)	172.0 (6)
O*w*—H*w*1···O2^{ii}	0.927 (9)	2.631 (3)	1.878 (1)	136.7 (1.3)
O*w*—H*w*2···O1^{iii}	0.949 (9)	2.780 (2)	1.960 (1)	143.6 (1.2)

Symmetry codes: (i) $2-x, -y, -z$; (ii) $x, \frac{1}{2}+y, \frac{1}{2}-z$; (iii) $2-x, \frac{1}{2}-y, \frac{1}{2}+z$.

The structural relationship between the two crystalline forms (AUA: anhydrous uric acid; UAD: uric acid dihydrate) perfectly explain the lattice similarities: a(UAD) = b(AUA) = 7.4; c(UAD) = c(AUA) = 6.3 Å; misfits of 0 and 2.3%, respectively (Boistelle & Rinaudo, 1981). The common metric is due to the fact that the ribbon projections in the planes normal to **b** in the dihydrate and normal to **a*** in the anhydrous form are nearly identical. This also beautifully explains why the orthorhombic (010) plane and the monoclinic (100) plane are the observed contact layers during epitaxial growth of the anhydrous form over the dihydrate form (Boistelle & Rinaudo, 1981). The two planes are structurally and metrically identical and the absence of the water molecule layer is the triggering factor for the overgrowth of anhydrous uric acid. Fig. 3 shows the

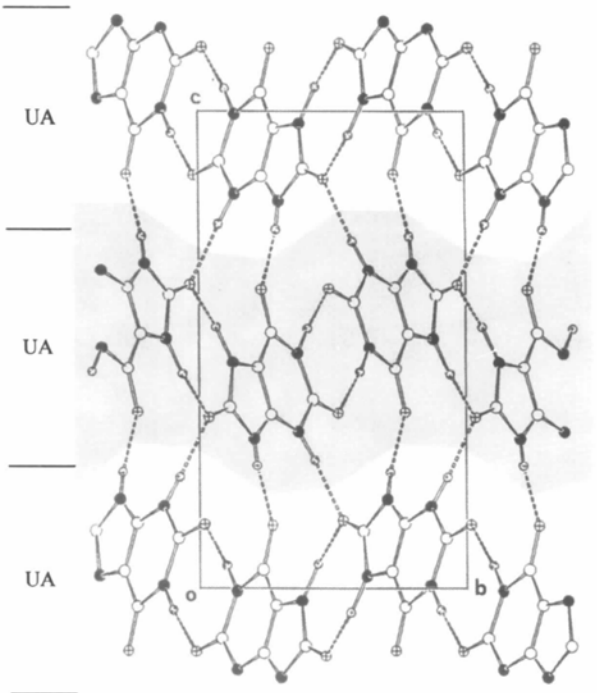

(*a*)

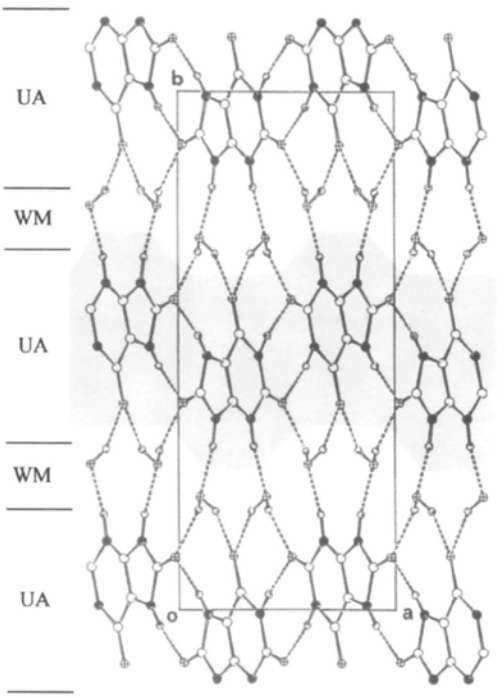

(*b*)

Fig. 2. Projection of the stuctures of (*a*) anhydrous uric acid and (*b*) uric acid dihydrate along [001]. The ribbons of doubly N—H···O connected molecules (UA) are highlighted and hydrogen bonds involving the water molecules (WM) are shown by dashed lines.

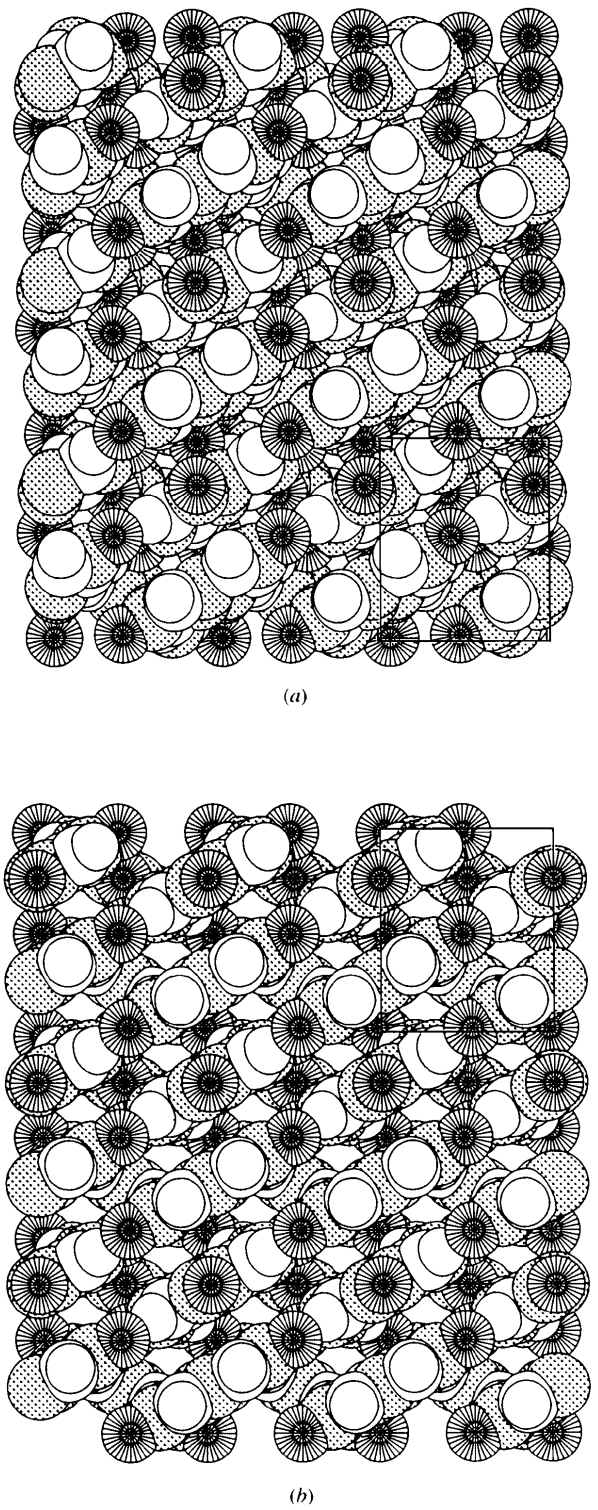

Fig. 3. Projections of the structures of (*a*) anhydrous uric acid down **a*** and (*b*) uric acid dihydrate down **b**, showing the molecular van der Waals surfaces. The atomic planes are identical and represent the contact plane for epitaxy between the two crystalline forms of uric acid.

crystal packing of the AUA and UAD phases in the *bc* and *ac* planes, respectively, showing the high similarity of the exposed faces. Moreover, the presence, in the dihydrate, of structural layers only formed by water molecules plus the possibility of a double orientation of the uric acid molecules in the ribbons due to the local disorder add a remarkable flexibility to the structure of uric acid dihydrate, with respect to the structure of the anhydrous form. Therefore, the epitaxial growth of UAD on AUA can occur, at least in principle, at a molecular level, with a random presence of intercalated water molecule layers in the pristine AUA matrix, and may result in a paracrystalline phase with a water/uric acid molecules ratio lower than 2:1. While such paracrystals have not been characterized to date (their existence being possibly hidden in the difficult growth of large single crystals of the pure UAD phase), mesoscopic intergrowths have indeed been observed in biomineralized urinary stones (Bastian & Grebhardt, 1974). Possibly, the observed metastability of some synthetic forms of UAD (Rinaudo & Boistelle, 1980) can be related to non-perfect stoichiometry.

It is worth remarking in this context that the observed epitaxial contact plane between anhydrous uric acid and whewhellite (Deganello & Coe, 1983; Deganello & Chou, 1984) is based on a lattice plane inclined *ca* 30° with respect to the *bc* plane of anhydrous uric acid. Based on the above discussion, it is to be expected that uric acid dihydrate might also show epitaxial contact with whewellite and even weddellite (Tazzoli & Domeneghetti, 1980). The long known metric relationships between uric acid dihydrate and the associated phases in human urinary stones (Lonsdale, 1968) are interpreted here by a precise structural model, whose flexibility and stacking disorder might bear implications for understanding the nucleation and growth processes in urolithiasis.

J. P. Lauriat and E. Elkaim are thanked for help during preliminary partial data collection at Lure. Funding from Italian CNR and MURST is acknowledged.

References

Altomare, A., Cascarano, G., Giacovazzo, C., Guagliardi, A., Burla, M. C., Polidori, G. & Camalli, M. (1994). *J. Appl. Cryst.* **27**, 435.

Artioli, G., Galli, E. & Ferrari, M. (1993). *Riv. Mineral. Ital.* **4**, 261–264.

Bastian, H. P. & Grebhardt, M. (1974). *Urol. Res.* **2**, 91–95.

Boistelle, R. & Rinaudo, C. (1981). *J. Cryst. Growth*, **53**, 1–9.

Bridge, P. J. (1974). *Mineral. Mag.* **39**, 889–890.

Deganello, S. & Chou, C. (1984). *Scanning Electron Microsc.* **II**, 927–933.

Deganello, S. & Coe, F. L. (1983). *Neues Jahrb. Miner. Monatsch.* **6**, 270–276.

Frank, M., Lazebnik, J. & DeVries, A. (1970). *Urol. Int.* **25**, 32–37.

Hesse, A., Schneider, H. J., Berg, W. & Hienzsch, E. (1975). *Invest. Urol.* **12**, 405–409.
Johnson, C. K. (1965). *ORTEP*. Report ORNL-3794. Oak Ridge National Laboratory, Tennessee, USA.
Larson, A. C. & Von Dreele, R. B. (1994). *GSAS Generalized Structure Analysis System*. Document LAUR 86-748. Los Alamos National Laboratory, New Mexico, USA.
Lonsdale, K. (1968). *Nature*, **217**, 56–58.
Lonsdale, K. & Mason, P. (1966). *Science*, **152**, 1511–1512.
Lonsdale, K., Sutor, D. J. & Wooley, S. (1968). *Br. J. Urol.* **40**, 33–36.
Mandel, N. S. & Mandel, G. S. (1980). *Contemporary Issues in Nephrology*, Vol. IV. Churchill & Levingstone.
Meyer, J. L., Bergert, J. H. & Smith, L. H. (1976). *Invest. Urol.* **14**, 115–119.
Prien, E. L. & Prien, E. L. Jr (1968). *Am. J. Med.* **45**, 654–672.
Rinaudo, C. & Boistelle, R. (1980). *J. Cryst. Growth*, **49**, 569–579.
Ringertz, H. (1965). *Acta Cryst.* **19**, 286–287.
Ringertz, H. (1966). *Acta Cryst.* **20**, 397–403.
Shirley, R. (1966). *Science*, **152**, 1512–1513.
Sutor, D. J. (1968). *Br. J. Urol.* **40**, 29–32.
Sutor, D. J. & Scheidt, S. (1968). *Br. J. Urol.* **40**, 22–28.
Sutor, D. J. & Wooley, S. E. (1972). *Br. J. Urol.* **44**, 532–536.
Tazzoli, V. & Domeneghetti, C. (1980). *Am. Mineral.* **65**, 327–334.